International Journal of Heat and Fluid Flow 63 (2017) 75–87

Contents lists available at ScienceDirect

International Journal of Heat and Fluid Flow

journal homepage: www.elsevier.com/locate/ijhff

Numerical simulation of drag-reducing channel flow by using bead-spring chain model

M. Fujimura[a], T. Atsumi[a], H. Mamori[b], K. Iwamoto[a,*], A. Murata[a], M. Masuda[c], H. Ando[d]

[a] Department of Mechanical Systems Engineering, Tokyo University of Agriculture and Technology, 2-14-26 Nakacho, Koganei-shi, Tokyo 184-8588, Japan
[b] Department of Mechanical Engineering, Tokyo University of Science, 6-3-1 Niijuku, Katsushika, Tokyo 125-8585, Japan
[c] National Institute of Advanced Industrial Science and Technology, 1-1-1 Higashi, Tsukuba-shi, Ibaraki 305-8568, Japan
[d] National Maritime Research Institute, 6-38-1 Shinkawa, Mitaka-shi, Tokyo 181-0004, Japan

ARTICLE INFO

Article history:
Available online 17 November 2016

MSC:
00-01
99-00

Keywords:
Drag reduction
Turbulent channel flow
Viscoelastic fluid
Discrete element model

ABSTRACT

Numerical simulations of the drag-reducing turbulent channel flow caused by polymer addition are performed. A bead-spring chain model is employed as a model of polymer aggregation. The model consists of beads and springs to represent the polymer dynamics. Three drag-reduction cases are studied with different spring constants that correspond to the relaxation time of the polymer. The energy budget is mainly focused upon to discuss the drag-reduction mechanism. Our results show that a decreasing pressure-strain correlation mainly contributes to strengthening the anisotropy of the turbulence. Furthermore, energy transport by the polymer models attenuates the turbulence. These viscoelastic effects on the drag-reducing flow are intensified with decreasing spring constant. By visualizing the flow field, it is found that this polymer energy transport is related to the orientation of the polymer.

1. Introduction

The addition of small amounts of polymer into wall turbulence can result in a large reduction in friction drag despite the scale of the individual polymer molecules being smaller than the viscous Kolmogorov scale. Since Toms (1948) discovered this effect, a great deal of research has been conducted for fundamental purposes. Several researchers (Cox et al., 1974; Dunlop and Cox, 1977; Vlachogiannis and Hanratty, 2004; Warholic et al., 1999; Wyatt et al., 2011) have focused on the role played by small aggregations, which are caused by entanglement between individual polymer molecules. Vlachogiannis and Hanratty (2004) visualized the aggregations by using fluorescence imaging and observed a larger drag reduction when the aggregations are present in the turbulent flow. Vlachogiannis et al. (2003) investigated the effect of polymer mechanical degradation by using a pump, which weakens the drag reduction effect. The mechanical degradation involves no significant changes in the molecular weight distribution, whereas destruction of aggregations occurs when the drag reduction effect is suppressed. Although it has become known that the effectiveness of polymer addition on the drag reduction effect depends on the presence of aggregations, the physical mechanism that causes the drag reduction has yet to be identified.

Recently, numerical simulation has become a handy tool for detailed investigations of turbulent flow. Numerous investigators have used constitutive models (e.g., the finite elastic nonlinear extensibility-Peterlin (FENE-P) model). In their constitutive equations, the polymer dynamics is represented in the Eulerian frame of reference (Bird et al., 1987). The dimensionless incompressible Navier–Stokes equation for the constitutive models can be written as

$$\frac{\partial u_i}{\partial t} + u_j \frac{\partial u_i}{\partial x_j} = -\frac{\partial p}{\partial x_i} + \frac{\beta}{\mathrm{Re}} \frac{\partial^2 u_i}{\partial x_j \partial x_j} + \frac{1-\beta}{\mathrm{Re}} \frac{\partial \tau_{ij}}{\partial x_j}, \quad (1)$$

where u_i, t, p, β, and τ_{ij} are the velocity, time, pressure, ratio of the solvent viscosity to the total viscosity, and viscoelastic stress, respectively. The subscript i $(= 1 \dots 3)$ denotes directions: $i = 1$ for the streamwise direction, $i = 2$ for the wall-normal direction, and $i = 3$ for the spanwise direction. For notational convenience, x_i is interchangeably used to denote the directions x, y, and z. The viscoelastic stress is derived on the basis of a dumbbell model, which is two beads linked by a spring as shown in Fig. 1a. For the FENE-P model, the polymer stress is given by

$$\tau_{ij} = \frac{1}{\mathrm{We}} \left\{ f(c) c_{ij} - \delta_{ij} \right\}, \quad (2)$$

where the conformation tensor c_{ij} is the phase average of the end-to-end vector of the dumbbell model, the Weissenberg number We is the ratio of the polymer relaxation time to the flow time scale, and $f(c) \equiv (\xi^2 - 3)/(\xi^2 - \mathrm{tr}C)$ is the Peterlin function, which is a

* Corresponding author.
E-mail address: iwamotok@cc.tuat.ac.jp (K. Iwamoto).

http://dx.doi.org/10.1016/j.ijheatfluidflow.2016.10.011

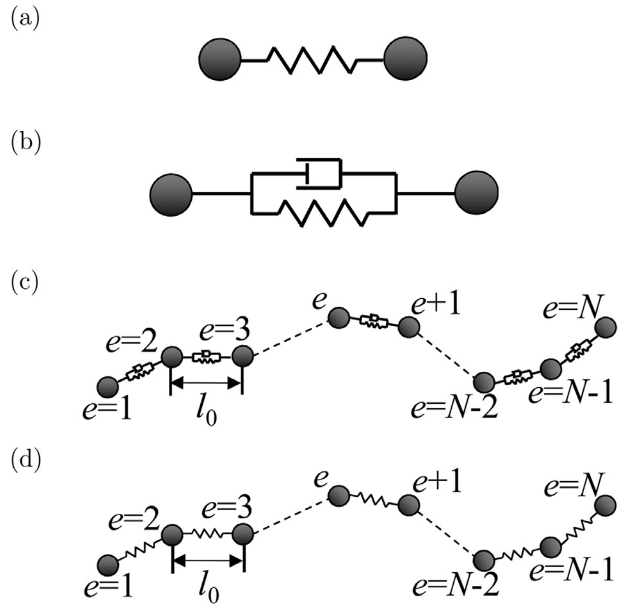

Fig. 1. Polymer models: (a) dumbbell model (used for deviation of constitutive models), (b) bead-spring-dashpot model, (c) bead-spring-dashpot chain model, and (d) bead-spring chain model. (a, b, and c are discrete element models).

closure approach to express the nonlinear spring with a maximum extensibility ξ. The evolution equation for the conformation tensor c_{ij} takes the form

$$\frac{\partial c_{ij}}{\partial t} = -u_k \frac{\partial c_{ij}}{\partial x_k} - c_{kj}\frac{\partial u_i}{\partial x_k} - c_{ik}\frac{\partial u_j}{\partial x_k} - \tau_{ij}. \tag{3}$$

Although constitutive models are somewhat coarse because of, e.g., the neglect of the inertia of the beads in the deviation process (Bird et al., 1987), Sureshkumar et al. (1997) adopted the FENE-P model with an artificial diffusion scheme and obtained results in qualitative agreement with experimental results. In more recent numerical investigations with constitutive models, the drag reduction mechanism has been discussed from a perspective of energy transport, which leads to a modification of the flow structure, strengthening the anisotropy of the turbulence (Dallas et al., 2010; Dimitropoulos et al., 2001; Dubief et al., 2004; Min et al., 2003; Thais et al., 2013; Tsukahara et al., 2011). Reynolds stress budgets were investigated by Dimitropoulos et al. (2001), who simulated drag-reducing turbulent flows with the FENE-P model. They observed that the magnitude of the pressure-strain correlation that redistributes the normal components of Reynolds stress from the streamwise to the wall-normal and spanwise directions is suppressed in viscoelastic fluid flow. Relationships between turbulent structures and the polymer in terms of turbulent kinetic energy transport were proposed through numerical simulations with the FENE-P model by Dubief et al. (2004), who found that the polymer stores energy around vortical structures and releases it into high-speed streak structures above the viscous sublayer. Recently, Thais et al. (2012) investigated the Reynolds number dependency up to the friction Reynolds number of Re_τ=1000. Thais et al. (2013) found that energy exchange term between polymer and turbulent kinetic energy is quite small for $y^+ <20$ with regard to a peak value for $y^+ \sim 35$ at Re_τ=1000 in contrast to Dallas et al. (2010) at a lower Reynolds number of $Re_\tau \sim 147.3$. Here, superscript of the plus denotes normalization by the kinematic viscosity of solvent ν and the friction velocity $u_{\tau 0} = \sqrt{\nu (du/dy)_{wall}}$.

These results with the constitutive models demonstrated some significant changes in energy transport. However, a continuous field of viscoelastic stress was considered in these studies, despite the fact that polymer aggregations locally interact with the turbulent structures (Cox et al., 1974; Dunlop and Cox, 1977; Vlachogiannis and Hanratty, 2004; Warholic et al., 1999; Wyatt et al., 2011). In the present study, we employed a discrete element model to simulate the aggregations. Kajishima and Miyake (1998) and Wang et al. (2012) introduced a bead-spring-dashpot model, a discrete element model shown in Fig. 1b. In this model, two beads are linked by a spring and a dashpot. The bead is a mass of polymer, the spring expresses elasticity, and the dashpot expresses internal viscosity. By using the dashpot, the numerical simulations can be stabilized. Wang et al. (2012) investigated the budget of turbulent kinetic energy by using bead-spring-dashpot models and observed that the models transport the energy from the buffer layer to the viscous sublayer. In studies by Kajishima and Miyake (1998) and Wang et al. (2012), verification of the natural spring length was not taken into account although physical interactions with the fluid are neglected between two beads. Subsequently, Utada et al. (2013) and Mamori et al. (2013) introduced a bead-spring-dashpot "chain" model, as shown in Fig. 1c. Here, N and l_0 represent the number of beads and the natural spring length, respectively. They investigated the dependence of the drag reduction rate on the natural spring length. When the natural spring length $l_0^+ < 4$, the drag reduction rate has no dependence on the natural spring length (cf. $l_0^+ \geq 15$ in the studies by Kajishima and Miyake (1998) and Wang et al. (2012)). In addition, by increasing the number of beads in the model, the large-scale aggregations can be simulated.

Our objective is to understand the mechanism of drag-reducing turbulent flow by polymer aggregations. In this paper, we introduce a simple model, a bead-spring chain model shown in Fig. 1d. Our model includes no dashpots which make the simulation stable, so the time step needs to become less than a factor of 5 times that of Utada et al. (2013) and Mamori et al. (2013) with dashpots. The polymer models are a rather crude representation. Therefore, to validate our model, the numerical results are compared with experimental results from particle image velocimetry (PIV) measurements conducted in our laboratory. To investigate how the flow structures are modified, the main focus is on the energy budget. By excluding dashpots, which cause energy dissipation, the model becomes similar to the dumbbell model used for derivation of the constitutive models. Thereby, we can discuss the energy budget through comparison to previous studies with the constitutive models.

The organization of this paper is as follows. Sections 2 and 3 describe the numerical simulations and experiments, respectively. In Section 4.1, basic results by the bead-spring chain model are compared with experimental results. Section 4.2 provides some statistics for the bead-spring chain models. Section 4.3 focuses on the energy budget with comparison to the results obtained from the constitutive models. Finally, conclusions follow in Section 5.

2. Numerical simulations

The properties of the bead-spring chain model are as follows:

1. Beads can be only in translational motion and the fluid force against bead motion is modeled as Stokes drag. The rotation and rear flow vortex of beads and springs are neglected.
2. It is assumed that the model is water soluble, so the density of fluid and beads are the same and gravity is neglected.
3. The spring is nonlinear because the polymer has an upper bound to its elongation.
4. Entanglement, collisions, and mechanical degradation of the models are neglected.
5. The fluid receives the reaction force of Stokes drag from the beads.
6. Brownian motion is neglected since the macro Brownian motion is suppressed when polymer molecules form aggregations.